Sensors and Actuators A 243 (2016) 71–80

Contents lists available at ScienceDirect

Sensors and Actuators A: Physical

journal homepage: www.elsevier.com/locate/sna

Mechanical behavior of strain sensors based on PEDOT:PSS and silver nanoparticles inks deposited on polymer substrate by inkjet printing

Michela Borghetti [a], Mauro Serpelloni [a,*], Emilio Sardini [a], Stefano Pandini [b]

[a] Dip. di Ingegneria dell'Informazione, University of Brescia, Brescia, Italy
[b] Dip. di Ingegneria Meccanica e Industriale, University of Brescia, Brescia, Italy

ARTICLE INFO

Article history:
Received 22 February 2016
Received in revised form 16 March 2016
Accepted 21 March 2016
Available online 22 March 2016

Keywords:
Strain sensor
Inkjet printing
Silver nanoparticles
PEDOT:PSS
Tensile tests
Mechanical behavior

ABSTRACT

Recently, inkjet printing technology has received growing attention as a method to produce low-cost large-area electronics, sensors, and antennas on polymer substrates. This technology relies on printing techniques to deposit electrically functional materials onto polymer substrates to fabricate electronic components or sensing elements. In this paper, we applied an inkjet printed technology for the development and characterization of films on a polymer substrate aiming at giving design considerations for the optimization of strain sensors or printed electronics obtained by inkjet printing. Two inks were tested over a polyimide substrate, a water-based conductive polymer, PEDOT:PSS, and a silver nanoparticles ink. Their sensing capabilities were investigated under tensile conditions and various strain histories (strain ramp; cyclic loading-unloading tests; application of constant strain over prolonged time) aiming at highlighting the correlation between electrical response, applied strain, time and mechanical histories. Furthermore, the mechanical viscoelastic response of the substrate was investigated under similar strain histories interpreting the results at the light of the substrate deformational characteristics and evaluating its influence.

1. Introduction

In recent years, sensors printed on polymer substrates represent an increasing area of research and development due to the growing demand for biosensors [1], artificial skin [2], chemical sensors [3], force [4] and strain sensors [5–9]. In particular, resistive strain sensors on polymeric substrates are employed, in general, for the measurement of forces [6], movements [7] and displacements [8]. Therefore, they are used in many different fields, and not least, in the biomedical field [9]. Novel systems have been recently developed adopting polymers instead of the more conventional strain gauges, leading to sensors based on conductive polymers [10], polymer composites [11], polymer elastomers [12], thermoplastics [12], epoxies [13]. As a benefit, sensors based on polymers allow the use of conventional and convenient polymer processing and post-processing techniques.

Resistive strain sensors are typically manufactured depositing a specific resistive ink on a polymer substrate. The polyimide films are often favored as substrate due to their high durability, the wide range of working temperatures and the stability to environmental factors [14]. Ink deposition can be easily carried out through simple and low cost printing technologies such as inkjet printing. This technique is one of the latest methodologies developed for the implementation of electronic components, and recently it is becoming increasingly popular, as evidenced by its adoption in numerous scientific publications [15–17]. This technique offers the advantage of being fast and relatively inexpensive, therefore suitable especially for the rapid development of prototypes to be tested. It also gives the possibility to deposit inks on various, rigid or flexible, substrates [15]. The main advantage of inkjet printed strain gauges, over the traditional ones, lies in their simple rapid prototyping process, the wide range of electric resistance, its compatibility with the mechanical properties of the material and its built-flexibility for the measurement of large deformations.

Two typical examples of conductive materials adopted as ink for inkjet-printing strain sensors are non-polymeric inks incorporating silver nanoparticles and the intrinsically conductive polymer poly(3,4-ethylenedioxythiophene)-poly(styrene sulfonate) (PEDOT:PSS). As example, a strain sensor based on silver ink, which could play a strategic role for electrodes and sensing structures due to the extremely low resistivity and mechanical properties, was recently proposed by Andò et al. [18]. On the other hand, piezoresistive sensors based on PEDOT:PSS can be used

* Corresponding author.
E-mail address: mauro.serpelloni@unibs.it (M. Serpelloni).

http://dx.doi.org/10.1016/j.sna.2016.03.021
0924-4247/

as strain sensors for various applications, also in the biomedical and health fields, due to its high biocompatibility [19]. Thermal and electrochemical stability and its high transparency [20] make PEDOT:PSS an interesting material, which also presents a certain versatility, such as the possibility of deposition on different substrates. Some examples of sensors manufactured with PEDOT:PSS deposited by inkjet printing are reported in Refs. [21] and [22], providing a characterization of their electrical and mechanical properties. In Ref. [22], a sensor based on PEDOT:PSS is adopted to measure the bending angle of knee flexion and wrist rotation. The results suggest that bending sensors fabricated by inkjet printing adopting PEDOT:PSS or silver nanoparticles ink offer many advantages with respect to other systems for human movement monitoring (inside and outside the human body), such as, the small footprint, low cost and versatility. However, to obtain satisfactory results from the use of these sensors, it is necessary to characterize properly their mechanical and electrical response, so to properly correlate, at the light of the substrate deformation, sensor response and movement.

In this paper, we present the results of tensile testing protocols, properly designed to evaluate the response of PEDOT:PSS and silver nanoparticles inks deposited by inkjet printing under monotonic and cyclic strain histories. The aim is to improve the knowledge on the design of strain sensors on polymer substrate or printed electronics manufactured by inkjet printing, with particular attention for what concerns the relationship between applied strain and measured electrical resistance, and stability of the response over time and for prolonged cyclic employ.

2. Preparation of sensing films

Two types of sensors were prepared and investigated, they were obtained depositing conductive inks on poly(imide) film (Kapton® HN DuPont [23]) by a proposed inkjet printing technique. For the first sensor type, the conductive layer is an ink based on silver nanoparticles. In particular, the ink is commercialized by Sigma Aldrich under the trade name 736465; it has a volume resistivity of 11 μW/cm, a nanoparticles content of 30–35% and a particle size less than 50 nm [24]. For the second type of sensor, the conductive layer is obtained by the deposition of PEDOT: PSS, Orgacon IJ-1005, marketed by AGFA-Gevaert [25] having 0.8% of solid part.

The employed film presents a thickness of 25 μm. The choice of polyimide was mainly motivated on its high adhesion to the chosen inks and biocompatibility [26]. Furthermore, it presents an enhanced thermal stability, when exposed to relatively high temperature, thanks to its high glass transition temperatures (about 360 °C). This is an important feature for the substrate, since sensors manufacturing process involves thermal treatment to promote the evaporation of the solvents. The thermal treatment helps towards increasing the conductivity of the ink and improving adhesion to the substrate: the moderate thermal expansion of the substrate on the range of temperature allows avoiding significant geometrical distortions of the substrate.

The sensors were made using the proposed inkjet printing method. A low-cost desktop printer has been used for the film depositions. The selected printer is one of the cheapest models of Epson, XP-215, having four separate cartridges with 128 nozzles for black and 42 nozzles for each color, and a print resolution up to 5760 × 1440 dpi.

Before the ink printing, the sheet of polyimide (155 × 21 mm^2) was cleaned by placing it in an ultrasonic bath of acetone for 15 min at room temperature. After cleaning, the strip was dried using dry compressed air. An additional oxygen plasma treatment (Colibrì, by Gambetti) under vacuum was carried out for the PEDOT:PSS-type substrates for 180 s at 35 W RF power in order to improve the adhesion between ink and polyimide. In fact, the plasma modifies chemical state of the polyimide surface, which becomes hydrophilic.

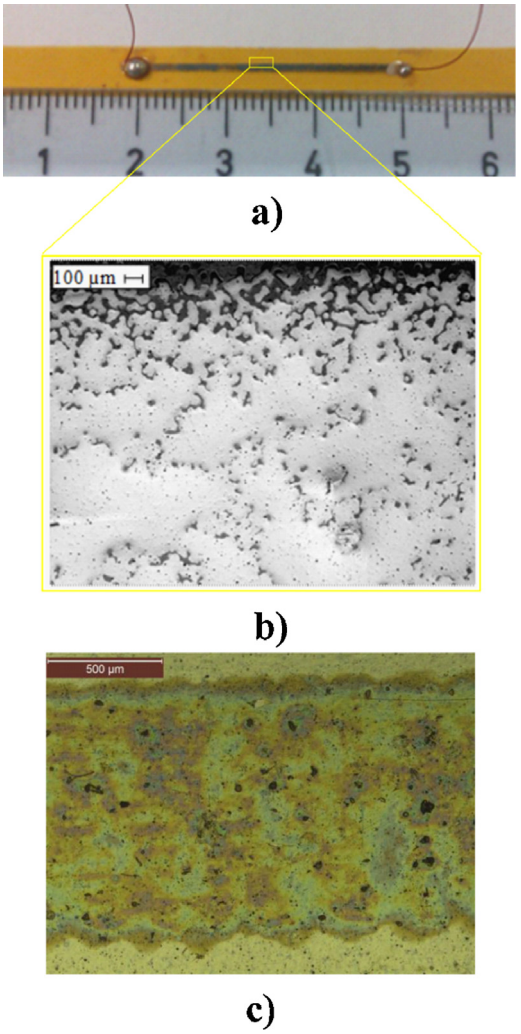

Fig. 1. (a) Example of a sensing strip for the tensile tests; observations at the optical microscope of the conductive track (b) for the silver nanoparticles ink and (c) for PEDOT:PSS.

An empty printer cartridge was refilled by the silver nanoparticles or PEDOT:PSS ink. Ink paths were created by repeating the printing process for three times for silver-based sensor and five for the PEDOT:PSS-based sensor, this ensures a good conductivity. After printing each of the layers, the sheet was dried in a static oven for 1 min at 50 °C to prevent the spread of ink with the following printing. After depositing all the layers, the sheet with devices in silver nanoparticles was placed in the oven for 30 min at 150 °C (6 min at 130 °C for PEDOT:PSS). To create contacts a silver paste (Dupont 5028) has been deposited manually and dried at 130 °C for ten further minutes, after which copper wires were soldered onto the silver paste, allowing measuring easily the electrical resistance.

A typical specimen prepared for the tensile testing, representative of the sensor, is represented in Fig. 1a, and is obtained by cutting rectangular strips (155 × 7 mm^2) from the printed sheet. This figure shows the sensitive track consisting of a single rectangular stripe of conductive ink, aligned with the specimen length and placed in the mid-span. For all the sensors, the conductive stripe has a nominal length of 30 mm and a nominal width of 1 mm.

We measured the resistance (R) of the deposited stripes with a 6½ digit digital multimeter. The average resistance is 6900 Ω of the stripes based on the PEDOT:PSS ink and 30 Ω of the ones based on

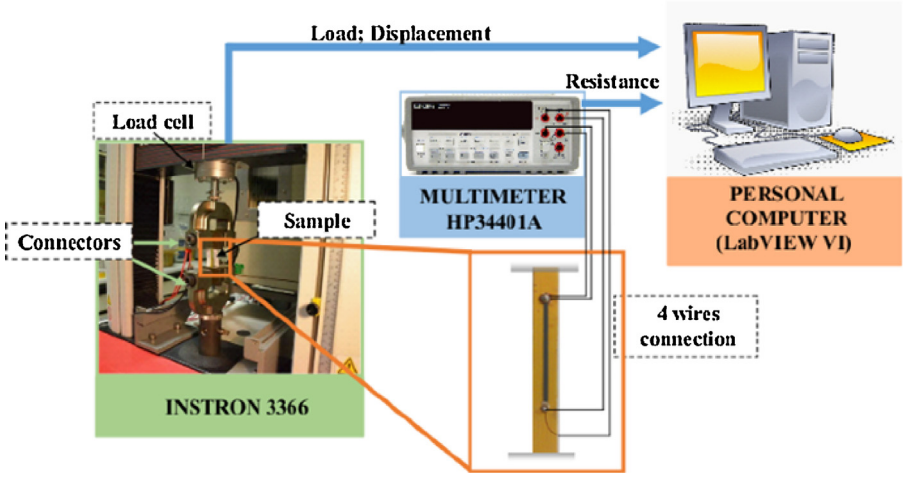

Fig. 2. Schematic representation of the experimental setup; the dynamometer (Instron 3366) is employed to apply specific deformation histories on the sample, measuring force and displacement, while the electrical resistance (R) is simultaneously measured by the multimeter. The two crocodile clamps are connected to the multimeter for resistance measurement.

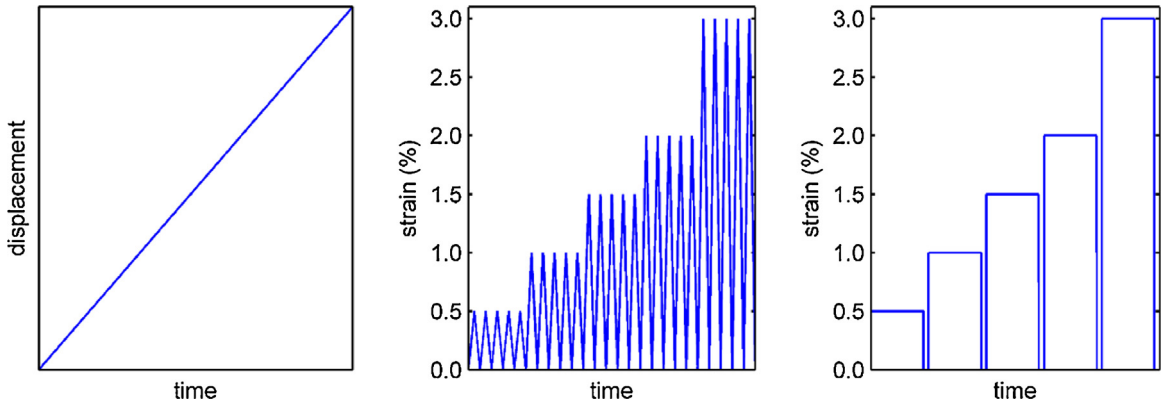

Fig. 3. Schematic representations of the three sets of tests: (a) a monotonic ramp at constant displacement rate; (b) loading–unloading cycles at various maximum levels of strains; (c) maintained strain levels for prolonged time.

the nanoparticle silver ink. We also measured the thickness (t) of the deposited inks with a stylus profilometer (Bruker Dektak XT). The average thickness of the PEDOT:PSS and of the nanoparticles silver is 400 nm and 600 nm, respectively.

Finally, we calculated the resistivity (ρ) of these two materials by using

$$R = \rho \times \frac{L}{W \times t} \quad (1)$$

where L and W are the length and the width of the stripe, respectively. We obtained a mean value of 92 μΩ m for the PEDOT:PSS and 0.60 μΩ m for the nanoparticle silver. The lower resistivity of the PEDOT:PSS with respect to the pristine PEDOT:PSS is justified by the presence of the diethylene glycol (DEG) in the liquid ink [27,28]. Indeed, DEG induces to create a highly conducting PEDOT:PSS network. The resistivity of the nanoparticle silver ink is usually 0.30–0.40 μΩ m, but in some cases it could be higher than 1 μΩ m [29,30]. The sintering process could be one of the reasons of a higher resistivity, as confirmed in the literature [31].

Fig. 1b and c refer to the conductive track obtained by silver nanoparticles and by PEDOT:PSS inks, respectively, as observed by an optical microscope.

3. Experimental setup

The experimental activity consisted in simultaneously monitoring strain and electrical signal when specific deformation histories were applied. A schematic block diagram of the experimental setup is displayed in Fig. 2.

The strain history was applied, under tensile configuration, by means of an electromechanical dynamometer (Instron, model 3366), equipped with a 500 N load cell and screw-type grips. In recent years, the standardization work for the mechanical characterization of printed electronics or sensors deposited on polymeric substrates has led to the publication of numerous standards (such as IEC62047 or IEC62899, etc.) also very specific to the particular field of application. However, in our research, the goal is to provide important design considerations for the optimization of sensors on polymeric substrates or printed electronics, or connections. Therefore, the samples that were manufactured were analyzed via protocols classically used for the characterization of polymeric materials in deformations. Tensile testing conditions were adopted since they allow providing the best description of the stress and strain conditions of the sensing portion of the film, whereas bending would have led to locally inhomogeneous stain levels throughout the specimen length.

A 6½ digits multimeter (Agilent 34401A) measured the electrical resistance using four wire connections. A personal computer (PC) with LabVIEW virtual Instrument (VI) controlled the Instron

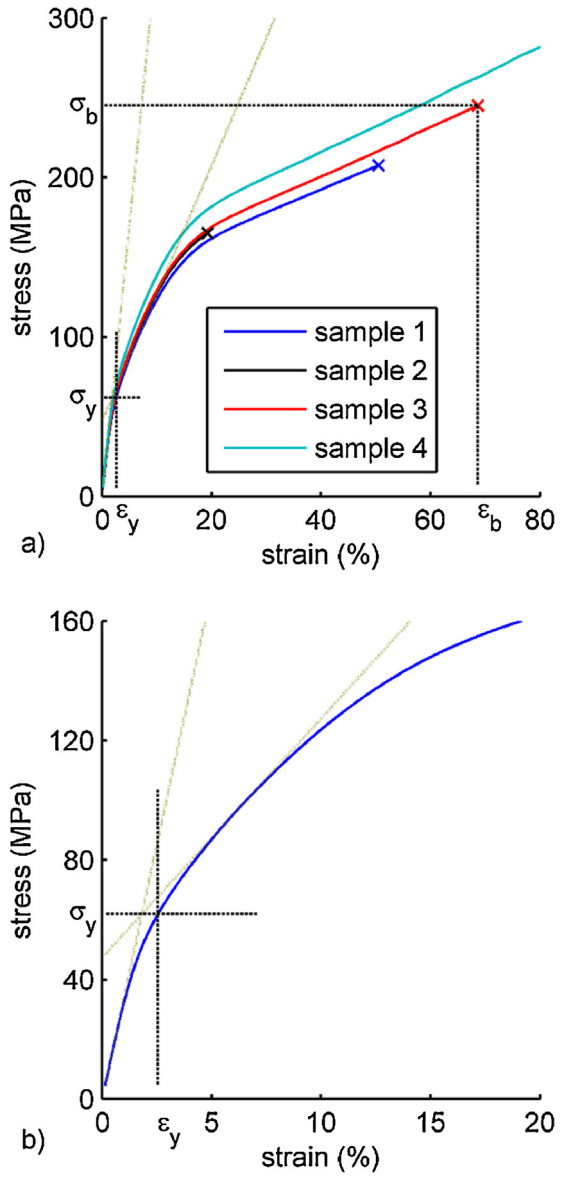

Fig. 4. (a) Stress vs. strain curves for the polyimide specimens; the two dotted lines represent construction curves for the determination of the yield point, the crosses corresponds to the break point; (b) Construction curves.

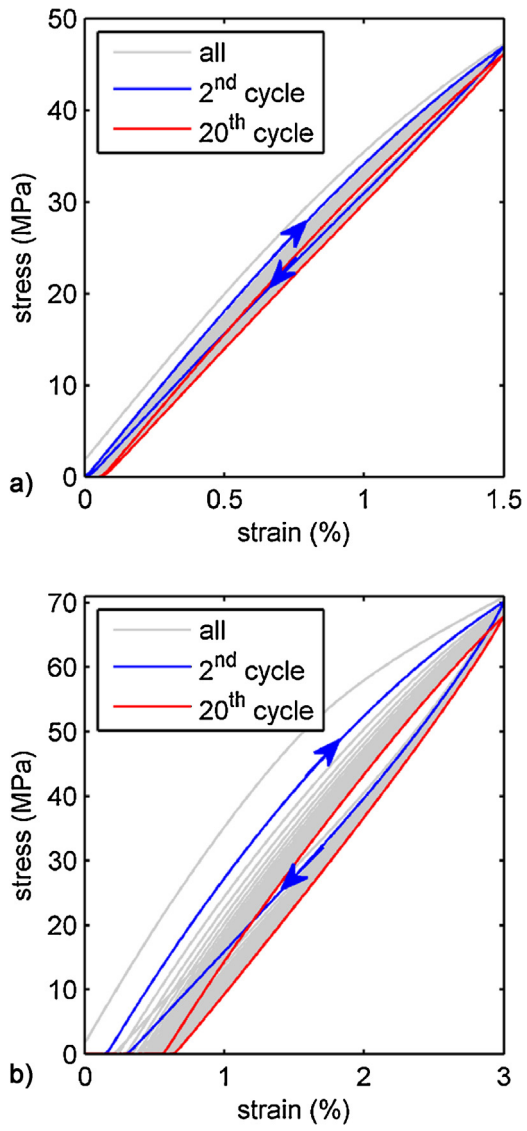

Fig. 5. Cyclic behavior of the substrate when the maximum deformation is (a) 1.5% and (b) 3%.

and acquired the data of load, displacement and resistance in real-time.

The correlation between stress, strain and variation of the electrical resistance were investigated under three deformation histories, schematically shown in Fig. 3. These tests were carried out on sensors, and, separately, also on neat polyimide film samples. i.e. polyimide strips without conductive ink, so to evaluate mechanical, viscoelastic and cyclic features of sensor's substrate. Neat polyimide samples were prepared as 160 mm long and 10 mm large rectangular strips. The gauge length (120 mm) of these neat samples is significantly longer than the length of the sensitive track in order to better characterize the intrinsic properties of the material and provide results free from effects of triaxiality to grips.

In the first type of test, strain ramp test (Fig. 3a), the mobile crosshead was moved at constant speed (10 mm/min) up to specimen failure.

The second type of test consists in cyclic loading-unloading tests, carried out by subjecting the sensor to 60 cycles for a given level of maximum strain. In the present research, the effect of the applied strain was investigated in subsequent cyclic experiments, increased the maximum strain at the end of each step, thus, the same specimen was subsequently subjected to 60 cycles at given level of strain, later increased for another set of 60 cycles, and up to the maximum strain. The explored set of strain was equal to 0.5%, 1%, 1.5%, 2% and 3%. The speed of the crossbeam was adjusted so that the tests had the same total duration of about 10 min; so the strain rate was set, respectively, 5.7%/min, 11.4%/min, 17.1%/min, 22.8%/min and 34.3%/min. After each step the specimen was unloaded and 10 min elapsed before the subsequent step.

The third type of test consists in applying a given level of strain and maintaining it for a given time, a testing protocol that corresponds to the polymer testing methodology known as stress relaxation test. Similarly to the cyclic test, the effect of the applied strain was investigated in subsequent relaxation step, increasing the level of deformation applied after each step. Progressively increasing deformations equal to 0.5%, 1%, 1.5%, 2% and 3% were applied, within loading ramp at constant speed (2 mm/min), and maintained for 12 min in each step, after which the specimen was unloaded and 10 min elapsed before the following step. In order to start with the specimen in pure tension, a preload of moderate entity (0.5 N) was applied on the sensor before each

Table 1
Mechanical properties of the polyimide substrate as determined in strain ramp tensile tests.

Polyimide characteristics	Value
E, Young modulus (GPa)	3.6 ± 0.2
σ_y, stress at yield (MPa)	66 ± 4
ε_y,strain at yield (%)	2.3 ± 0.4
σ_b, stress at break (MPa)	230 ± 50
ε_b, strain at break (%)	55 ± 27

ramp, allowing controlling properly the strain value applied in each step.

The stress value was calculated as engineering stress, by normalizing the measured load to the initial cross-section of the sample. For this calculation, the thickness of the polyimide substrate (25–30 μm) was considered; the thickness of the conductive layer, equal to few hundred of nanometer, was considered negligible. The strain was expressed as engineering strain, which is the ratio between the elongation of the specimen and the initial length between grips.

4. Experimental results

4.1. Mechanical behavior of the polyimide substrate

Mechanical tests were preliminarily carried out on four specimens of the polyimide substrate in order to evaluate its mechanical response to the various deformation histories.

In Fig. 4a, the stress vs. strain relationship measured along a monotonic strain ramp at constant displacement rate is reported, and the four specimens show a good repeatability (the deviation standard is about the 5%). This test allowed evaluating the material stiffness as well as its yield and break point, whose values are reported in Table 1.

At the lower strains, the specimens display a linear increasing trend, on which the Young modulus, E, was evaluated; deviations from this trend are found at higher levels of strains, and they are displayed as two subsequent reductions of the curve slope before final break. The first deviation from the linear trend is assumed representative of the yield phenomenon. The values of yield stress, σ_y, was calculated as the stress at the intersection of two lines interpolating the linear trends displayed before and after this deviation, as schematically sketched in Fig. 4b; the yield strain, ε_y, was evaluated on the stress vs. strain curves in correspondence of the yield stress. The values of stress and strain at break (σ_b and ε_b, respectively) were evaluated as the coordinates of the maximum point of the curve before the abrupt fall of stress occurring at break. The results suggest that the substrate material undergoes yielding and localized plastic deformation already at strain levels equal to about 2.3%. Therefore, in particular for cyclic loading-unloading tests, the maximum level of adopted strain never exceeded 3%, whereas the minimum value of 0.5% was adopted in order to assure a reliable displacement control by means of the dynamometer.

Cyclic loading-unloading tests were carried out to study the substrate response under this strain history, and for various levels of maximum strains, with the specific aim to highlight hysteresis in the stress *vs.* strain correlation for repeated cycles and to evaluate the accumulation of residual deformation at the end of each cycle. Fig. 5 shows the entire output of the whole cyclic test (up to 20 cycles, lasting about 15 min); in particular, Fig. 5a refers to a maximum strain equal to 1.5%, whereas Fig. 5b to a strain equal to 3%, corresponding to values right below and above the yield strain, respectively.

For both strain levels, a hysteretic response is evidenced, as confirmed by the area comprised between loading and unloading. As the number of cycles increases, a progressive reduction of this area and an overlapping of the loading-unloading cycles occur. The results show that under these conditions the material undergo to a large evolution of stress-strain correlation in the first cycle, tending only above 10 cycles to a common trend. Further, the presence of a residual deformation at the end of each cycle is shown. This is not so relevant for maximum deformation levels up to 1.5% (for this level of strain the residual deformation is about 0.05% after the 1st cycle and approaching 0.1% after the 20th cycle). It becomes more important for higher levels of strain (in the case of the highest strain explored the residual strain increases from 0.3% to 0.6% during the test).

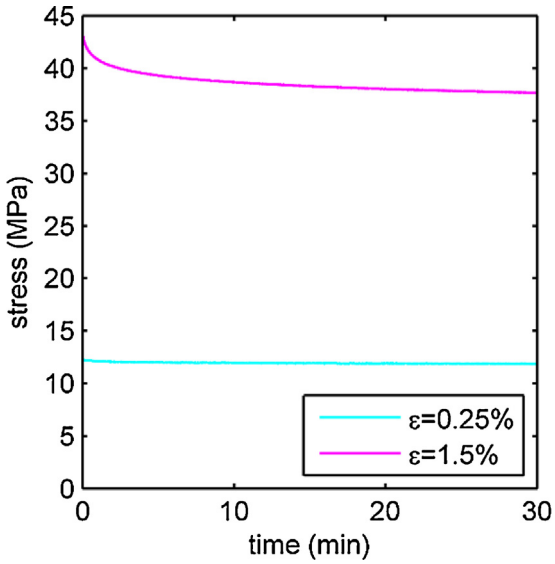

Fig. 6. Stress relaxation tests on the neat polyimide film under two levels of strains.

The stress relaxation tests, carried out by subjecting the specimen at a constant strain and monitoring the stress decreasing in time for 30 min, provided the results reported in Fig. 6, for two levels of strain (0.25% and 1.5%, respectively), both chosen below the evaluated yield strain. At all the applied strains, the expected stress reduction is found, but whereas the effect is moderate (i.e. a

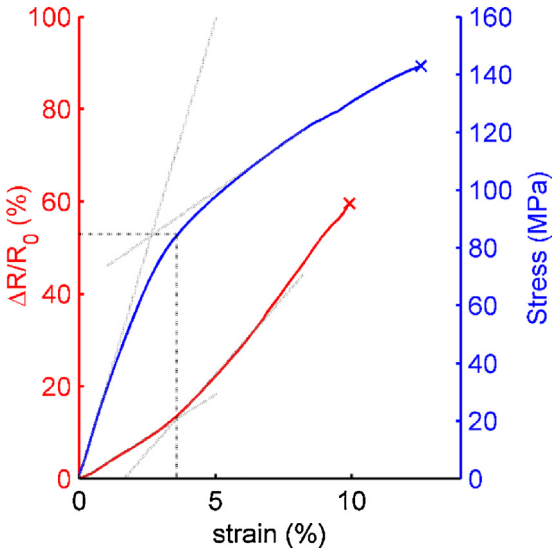

Fig. 7. Normalized resistance change ($\Delta R/R_0$) as a function of strain and simultaneously measured stress vs. strain curve for the sensor with silver particles ink ($R_0 = 31\ \Omega$); the dotted lines are construction lines to better evaluate the change of the slopes, while the dashed lines define the level of strain at which the change occurs.

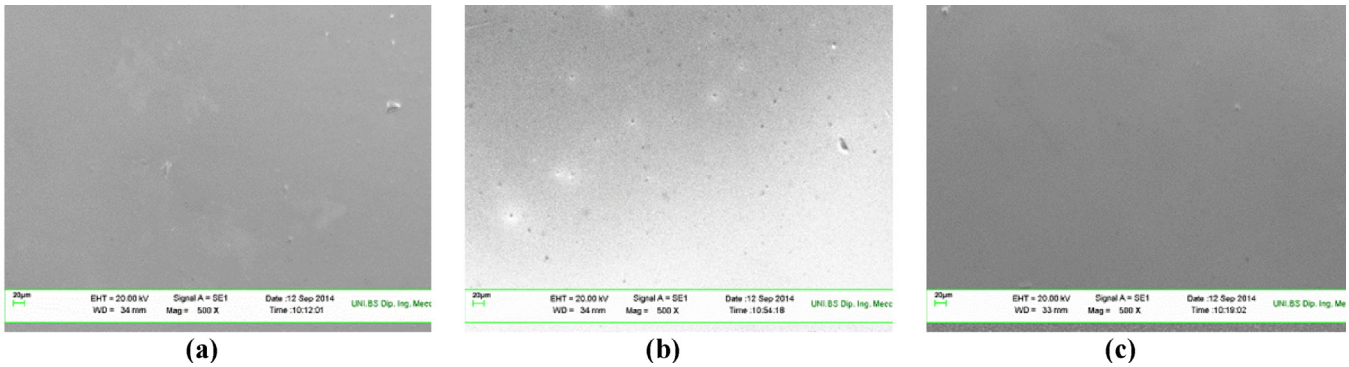

Fig. 8. SEM analysis for the microcrack detection when the stripes based on nanoparticle silver ink are (a) unstressed, (b) elongated at 1%, (c) elongated at 5%. No cracks are visible in the elongated stripes.

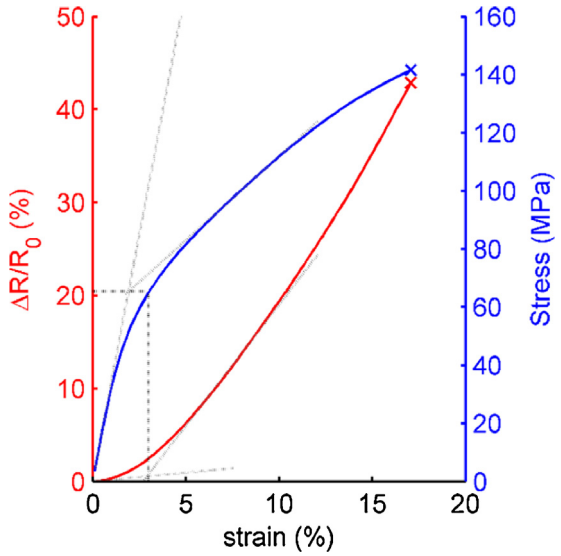

Fig. 9. Normalized resistance change ($\Delta R/R_0$) and stress evolution of strain, and gauge factors ($R_0 = 6890\ \Omega$); the lines represent the specific levels of strain for the resistance variation rate and the strain at yield (from the stress curve).

decrease of about 2.8% within 30 min) for the lowest strain, at 1.5% the decrease becomes markedly more significant (i.e. about 13%), faster and it does not seem to approach a stable plateau within the test time, as a probable consequence in the nonlinear viscoelasticity regime.

4.2. Sensors responses in tensile ramp tests

Sensors responses to a quasi-static tensile ramp (Fig. 3a) are reported in Figs. 7 and 9, where the specimens are deformed at a constant strain rate up to the specimen failure.

In Fig. 7, the sensor behavior with silver nanoparticles ink is shown in terms of normalized resistance change, $\Delta R/R_0$, as a function of strain ($R_0 = 31\ \Omega$); also the stress vs. strain curve, simultaneously measured on the sensor, is reported.

The normalized resistance change shows an evident increasing dependence on strain, displayed as a subsequence of two almost linear trends with different slopes. At levels of strain of about 4%, in fact, the initial linear trend gradually approaches a second trend with a higher slope. Interestingly, by comparing this trend with the stress vs. strain relationship, it is suggested that the change in slope takes place in the region near to yield occurrence. Finally, at higher strains, but well before specimen failure, the resistance presents an abrupt increase of many orders of magnitude, (conditions of "overload"). The last deformation value acquired, which is about 8–10%, can be adopted to estimate the maximum limit of sensitivity.

The increasing dependence of $\Delta R/R_0$ with the strain can be also expressed in terms of an increase of gauge factor, which was easily evaluated as slope of the $\Delta R/R_0$ vs. strain curve, assuming values of $G_1 = 3.72$ in the first portion of the curves, and becoming almost twice ($G_2 = 6.7$) afterwards. The increase in resistance with strain can be ascribed to a change in geometry of the conductive track, which increases its length and reduces its width, as well as to a change in resistivity. In particular, the significant change of slope occurring in correspondence to the yield point, and the associated localization of strain, could suggest that yielding is at the basis of the resistance variation, as a consequence of damages to the conductive path at the microscale. The phenomenon can be considered increasing with strain until localized breaking of the sensitive track or detachments of the sensitive track with the silver connection lead to the overload. Similar results were obtained by Valeton et al. [32], who, for a sensor obtained by depositing a silver-based ink on a PET (poly(ethylene terephthalate)) substrate, interpreted the change in electrical resistance induced by tensile strain as a consequence of microcracks on the conductive track, and the asymptote at high deformations to excessive microcracking.

In order to verify the presence of such microcracks on the stretched sensors, the morphology of the conductive tracks was investigated, using a scanning electron microscope (SEM) and an optical microscope. No significant morphological changes were found for strain levels above and below the yield point with respect to the undeformed specimens. These results seem to suggest that such path alteration, if any, could be ascribed to very localized strain at the substrate-track interface but do not involve film cracking at the surface. As a representative case, the SEM analyses on an unstressed stripe, on a stripe elongated at 1% and at 5% image are shown in Fig. 8. Clearly, further experiments are required to better understand what is occurring in the conductive path.

In Fig. 9, the experimental results for PEDOT:PSS-based sensor are reported. The normalized resistance variation shows an increasing dependence on strain, as in the case of silver ink, but differing in terms of curve shape, which displays a smoother and continuous increase of slope, attaining a linear trend only for strain levels above yielding. Interestingly, the curve shows an evident curvature, which closely resembles the stress vs. strain evolution, in particular in the yield region. Furthermore, the change in strain is evaluated on the whole strain scale up to failure, so that the sensing capabilities of the sensors are limited only by the substrate ductility, probably due to the higher ductility of the PEDOT:PSS tracks with respect to those in silver nanoparticles.

The pronounced curvature of the $\Delta R/R_0$ vs. strain at low strain levels inhibits a proper evaluation of the gauge factor on these strain levels, whereas that at higher strains can be calculated more eas-

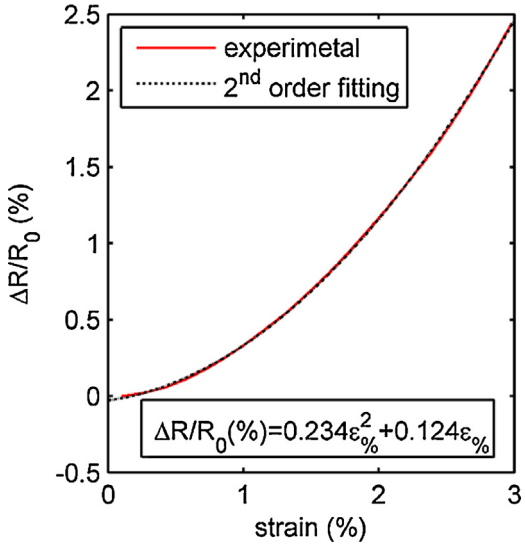

Fig. 10. Experimentally measured normalized resistance change ($\Delta R/R_0$) as a function of strain and fitting with a second order polynomial curve.

ily. Nevertheless, to compare the sensor performances, the value of gauge factors below and above the yield points (G_1 and G_2, respectively) were attempted. The value of G_1, defined as the slope of tangent at the curve for strains below 3%, is seen to vary between 0.19 and 1.59; the value of G_2, evaluated on the last part of the curve (above 5%, as shown in the construction line in Fig. 9) is about 2.6. Both the values of gauge factors on corresponding strain regions are seen to be lower than those found for the silver nanoparticles ink.

In this case, in contrast to the bilinear trend found for the silver nanoparticles ink-based sensors, the relationship between resistance variation and strain can be described by a second-order polynomial equation, as shown in Fig. 10. It seems to suggest that the resistance response should be researched in a change of the electrical conductivity depending on the applied strain; the conductive PEDOT grains [19] change their interdistance under different levels of strain.

The calibration curve of the sensor based on PEDOT:PSS could be approximated to a linear curve if it is required by the specific application. Criteria for selecting of the two calibration points minimizing the error could be adopted successfully in this case, as proposed by Pallàs-Areny et. al [33].

4.3. Sensors response under cyclic and static applications of strain

The sensor responses to a cyclic application of progressively increasing levels of stress (Fig. 3b) are presented for the system printed with silver nanoparticles ink in Fig. 11. The graphs in Fig. 11a and b show the normalized variation of the electrical resistance within the whole cyclic tensile test for the minimum (1%) and the maximum (3%) level of applied strain. At both levels of strain, the curves are characterized by two important drifting phenomena: i) hysteretical effects in the $\Delta R/R_0$ vs. strain dependence, which becomes less important as the cycles increase; ii) a vertical shift of the $\Delta R/R_0$ vs. strain curves as the cycles increase. Furthermore, the sensor at unloading does not fully recover the applied deformation; although, the value of minimum deformation is lower than 0.1%, in the last part of the unloading segment the sensor tends to bend, presenting a buckling effect; this effect becomes more important as the applied strain and the number of cycles increasing. This determines the presence of the plateau shown for low strain levels in Fig. 11b. This effect is clearly dictated by the fact that the sensor

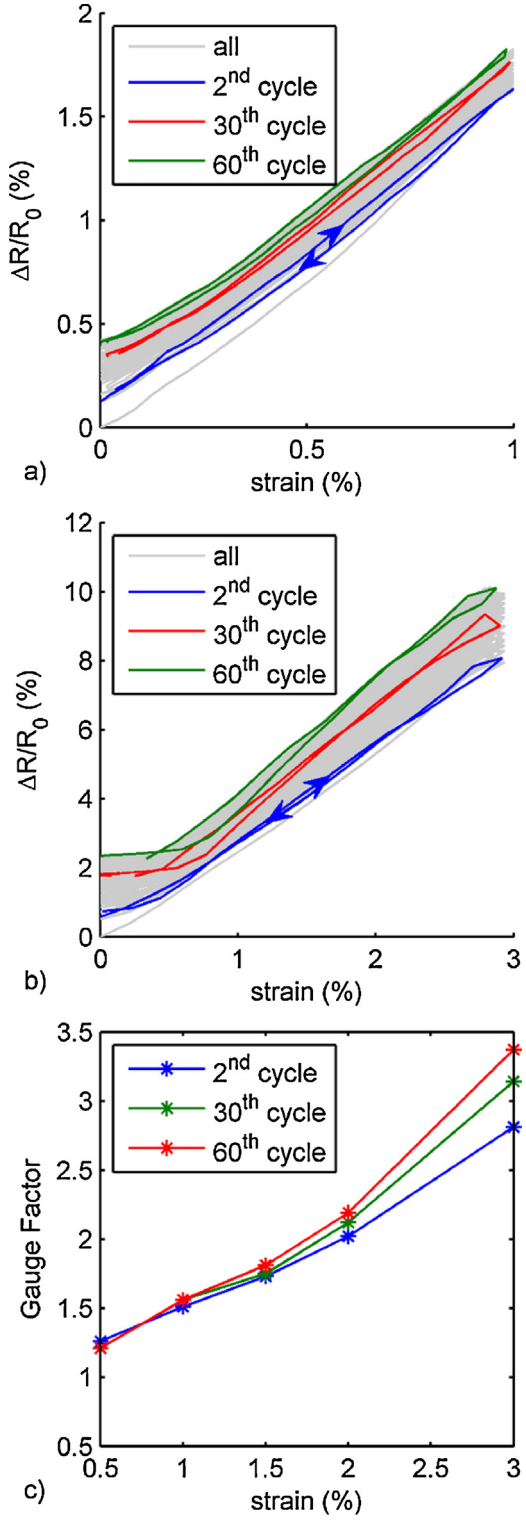

Fig. 11. Response of the silver nanoparticles ink sensor under the application of loading-unloading cycles at a given maximum strain value, corresponding to (a) 1.5% and (b) 3%; grey curves represent the continuous reading of the sensor on all cycles and the curves corresponding to the 2nd, 30th and 60th cycle are highlighted. (c) Evolution of the gauge factor with the cycles and the maximum strain applied.

response is important under stretching, but not under compression or flexure. As a consequence, there is a reduction of sensor sensitivity to small levels of deformation, the extension of this plateau of poor sensitivity increases with the number of cycles and also with the maximum deformation applied during the test. In fact, this phe-

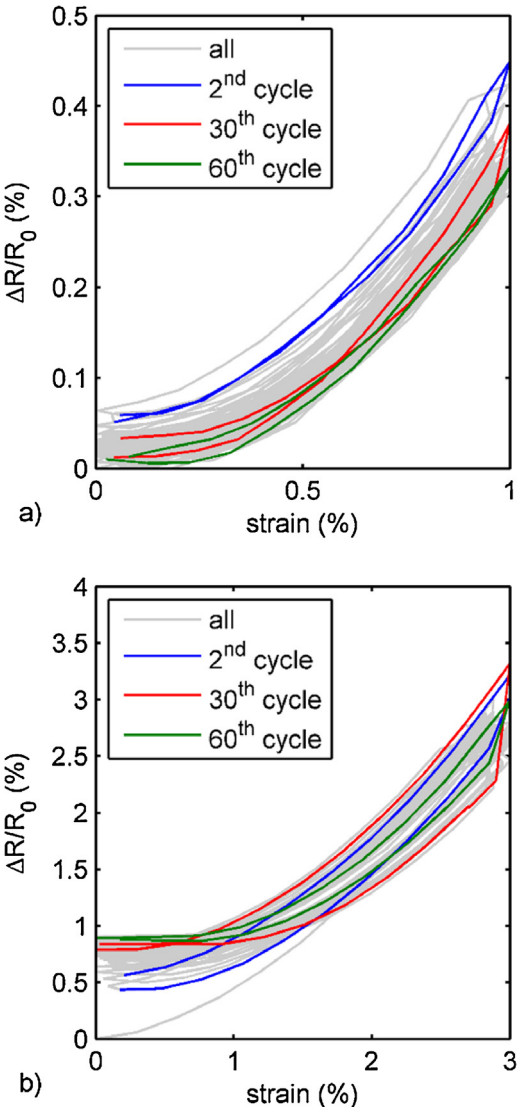

Fig. 12. Response of the PEDOT:PSS ink sensor under the application of loading-unloading cycles at a given maximum strain value, corresponding to (a) 1% and (b) 3%; grey curves represent the continuous reading of the sensor on all cycles, while in colors are highlighted the curves corresponding to the 2nd, 30th and 60th cycle.

Table 2
Average gauge factor for various levels of maximum applied strain and various cycles.

	Gauge Factor		
Strain (%)	2nd cycle	30th cycle	60th cycle
0.5	1.26	1.21	1.21
1.0	1.51	1.56	1.56
1.5	1.73	1.75	1.81
2.0	2.02	2.12	2.19
3.0	2.81	3.14	3.37

nomenon is well evidenced for the highest levels of strains, but it starts to become relevant at maximum deformation levels of 2%, i.e. in proximity of the yield strain.

To provide an evaluation of the overall sensor capabilities, we also tried to establish an average value of the gauge factor, calculated as average slope of the single cycle, and the results are reported in Table 2 and in Fig. 11c, with particular reference to the 2nd, 30th and 60th cycle. The gauge factor value is representative of the average sensitivity on the whole strain intervals; for this reason,

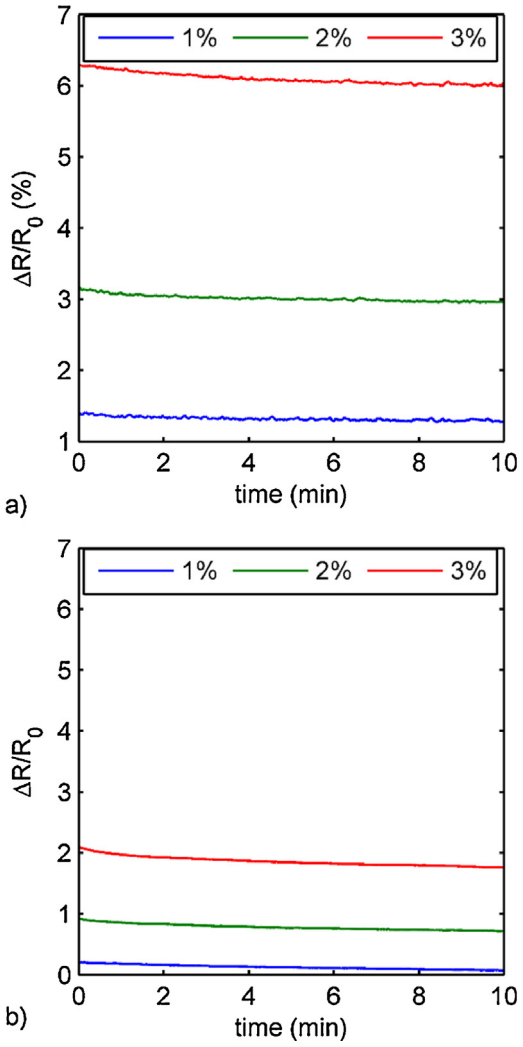

Fig. 13. Response of the sensors with silver particles-based ink (a) and PEDOT:PSS-based ink (b), when a constant strain value is applied and maintained constant in time.

as the maximum strain increases, higher values of gauge factor are found, due to influence of the high strain response. In any case, it is worthwhile to note that for a deformation up to 1.5%, there is no specific dependence of the gauge factor from the number of cycles. Such a dependence on the number of cycles becomes appreciable for maximum strains equal to 2%, and it becomes evident in the tests at 3%. This effect, having place in correspondence to the yield strain, can also be a feasible index for a marked material damage of the substrate or the conductive path, as underlined for the tensile tests.

The PEDOT:PSS ink-based sensors were subjected to cyclic tests under the same conditions and the results are reported in Fig. 12a and b, for maximum deformation levels of 1% and 3%, respectively.

The sensors response under the application of a constant strain (Fig. 3c) was investigated, in order to understand whether the material presents a drift in the response with time, and whether such drift is affected by various strain regimes. In Fig. 13, the results for the sensors printed with silver nanoparticles-based ink and PEDOT:PSS-based ink, respectively, are reported. The curves represent the evolution of $\Delta R/R_0$ over time; R_0 is the resistance of the undeformed sensor. Both sensors undergo a reduction in resistance with time; furthermore, this effect is more evident for higher applied strains, and it seems that the PEDOT:PSS-based sensors are more prone to such an effect. The reasons behind such effect are

not clear, and we suppose a variation in shape of the conductive track during time (for example due to the variation over time of Poisson's ratio or with effects in micro-localized deformation) or to an alteration of conductive capacity, for example due to exposure to the external environment and atmospheric moisture. Further, it is interesting underline that the reduction in resistance accompanies the stress decrease showing a very close similarity with it. In any case, the resistance decrease is relatively small for the silver-based ink, which shows an overall reduction of 0.3% at the highest applied strain; for the PEDOT:PSS-based sensors such reduction is more important, and it attains values of about 4%.

This is compared with sensors at rest for 30 min indicating that the resistance decrease measured in the tests with constant deformation, even though limited, is caused by the behavior of the sensor during the tests and it is not exclusively the result of the drift that the sensor would even have if unloaded.

5. Conclusions

This paper provides a mechanical characterization of strain sensors realized by inkjet printing on a polymer substrate conductive tracks based on a PEDOT:PSS-based ink or on an ink containing silver nanoparticles. In all the tests, it was possible to highlight the close correlation of proportionality that exists between the deformation and resistance change. In particular, from the ramp tests obtained with silver-ink sensors, the correlation can be represented as the series of two subsequent linear trends, whereas this behavior is different with respect to sensors realized with PEDOT:PSS, in which the correlation can be represented as a second order polynomial function. The gauge factor for silver-ink sensors is about 3.7, whereas for PEDOT:PSS-ink sensors the gauge factor is less than 1. The increase of resistance with the deformation is not ascribed solely to the dimensional variation of the conductive track, but also to a change of the resistivity with deformation. Furthermore, the application of a constant deformation over time has revealed a progressive decrease of the resistance. Such drift is modest, the resistance variation, calculated with a deformation maintained at 3%, is about 0.3% if compared to the initial resistance value. Finally, the application of loading-unloading cycles showed: a) a hysteresis in the sensor response, b) a progressive drift of the resistance towards greater values with increasing number of cycles and c) the formation, with low deformation values, of a plateau of poor sensitivity. These phenomena occur in a limited mode up to deformations of 1.5–3% and these are evident in the tests in which the sensor is deformed up to 3%.

The substrate influence on the sensor behavior has been experimentally verified. The high rigidity of the polyimide causes a low slope of the first portion of the curve resistance-stress obtained in ramp deformation. In the future, aiming at obtaining more versatile strain gauge sensors, which work for example on a larger scale of deformation, elastomeric materials can be studied as substrate. These substrates can eliminate the problem of the yield, reduce the stiffness (and thus increase the sensitivity to the stress) and mitigate the phenomenon of stress relaxation, although it is necessary to find the conditions for a good wettability to the conductive ink. For the elastomeric substrate, the PEDOT:PSS ink could be a better alternative than the nanoparticle silver ink for fabricating sensors, even if the gauge factor is lower and the resistance drift is more evident. Indeed, whereas the last deformation of the stripes based on silver is 8–10% (before the specimen failure), the one of the PEDOT:PSS stripes acquired by the tensile ramp test is 17% which corresponds to the strain at break.

References

[1] Y. Sun, K. He, Z. Zhang, A. Zhou, H. Duan, Real-time electrochemical detection of hydrogen peroxide secretion in live cells by Pt nanoparticles decorated graphene–carbon nanotube hybrid paper electrode, Biosens. Bioelectron. 68 (2015) 358–364.

[2] Y. Huang, W. Dong, T. Huang, Y. Wang, L. Xiao, Y. Su, Z. Yin, Self-similar design for stretchable wireless LC strain sensors, Sens. Actuators A 224 (2015) 36–42.

[3] R. Ghosh, A. Singh, S. Santra, S.K. Ray, A. Chandra, P.K. Guha, Highly sensitive large-area multi-layered graphene-based flexible ammonia sensor, Sens. Actuators A 205 (2014) 67–73.

[4] R.D.P. Wong, J.D. Posner, V.J. Santos, Flexible microfluidic normal force sensor skin for tactile feedback, Sens. Actuators A 179 (2012) 62–69.

[5] J.-H. Kim, Y. Liang, S. Seo, Patchable thin-film strain gauges based on pentacene transistors, Org. Electron. 26 (2015) 355–358.

[6] C.-W. Ma, L.-S. Hsu, J.-C. Kuo, Y.-J. Yang, A flexible tactile and shear sensing array fabricated using a novel buckypaper patterning technique, Sens. Actuators A 231 (2015) 21–27.

[7] S.-H. Bae, Y. Lee, B.K. Sharma, H.-J. Lee, J.-H. Kim, J.-H. Ahn, Graphene-based transparent strain sensor, Carbon 51 (2013) 236–242.

[8] A. Bessonov, M. Kirikova, S. Haque, I. Gartseev, M.J.A. Bailey, Highly reproducible printable graphite strain gauges for flexible devices, Sens. Actuators A 206 (2014) 75–80.

[9] G. Saggio, Electrical resistance profiling of bend sensors adopted to measure spatial arrangment of the human body, Proceedings of the 4th International Symposium on Applied Sciences in Biomedical and Communication Technologies (2011), article No. 5.

[10] J.N. Pereira, P. Vieira, A. Ferreira, A.J. Paleo, J.G. Rocha, S. Lanceros-Mendez, Piezoresistive effect in spin-coated polyaniline thin films, J. Polym. Res. 19 (2012) 0–6.

[11] A. Ferreira, J.G. Rocha, A. Anson-Casaos, M.T. Martınez, F. Vaz, S. Lanceros-Mendez, Electromechanical performance of poly(vinylidene fluoride)/carbon nanotube composites for strain sensor applications, Sens. Actuators A 178 (2012) 10–16.

[12] P. Costa, J. Silva, V. Sencadas, R. Simoes, J. Viana, S. Lanceros-Mendez, Mechanical: electrical and electro-mechanical properties of thermoplastic elastomer styrene–butadiene–styrene/multiwall carbon nanotubes composites, J. Mater. Sci. 48 (2013) 1172–1179.

[13] A. Ferreira, P. Cardoso, D. Klosterman, J.A. Covas, F.W.J. van Hattum, F. Vaz, S. Lanceros-Mendez, Effect of filler dispersion on the electromechanical response of epoxy/vapor-grown carbon nanofiber composites, Smart Mater. Struct. 21 (2013) 075008.

[14] H. Ohya, V.V. Kudryavsev, S.I. Semenova, Polyimide membranes: applications, fabrications and properties, CRC Press, 2016, pp. 1997.

[15] B. Andò, S. Baglio, All-Inkjet printed strain sensors, IEEE Sens. J. 13 (2013) 4874–4879.

[16] N. Komuro, S. Takaki, K. Suzuki, D. Citterio, Inkjet printed (bio)chemical sensing devices (2013) anal, Bioanal. Chem. 405 (2013) 5785–5805.

[17] G. Cummins, M.P.Y. Desmulliez, Inkjet printing of conductive materials: a review, Circuit World 38 (2012) 193–213.

[18] B. Andò, S. Baglio, S. La Malfa, G. L'Episcopo, All inkjet printed system for strain measurement, IEEE Sens. Conf. 2011 (2011) 215–217.

[19] M. Yang, Y. Zhang, H. Zhang, Z. Li, Characterization of PEDOT:PSS as a biocompatible conductive material, in: Proceedings of the 10th IEEE International Conference on Nano/Micro Engineered and Molecular Systems (NEMS), Xi'an, China, 2015, pp. 149–151.

[20] M. Hokazono, H. Anno, N. Toshima, Thermoelectric properties and thermal stability of PEDOT:PSS films on a polyimide substrate and application in flexible energy conversion devices, J. Electron. Mater. 43 (2014) 2196–2201.

[21] Y. Seekaew, S. Lokavee, D. Phokharatkul, A. Wisitsoraat, T. Kerdcharoen, C. Wongchoosuk, Low-cost and flexible printed graphene–PEDOT:PSS gas sensor for ammonia detection, Org. Electron. 15 (2011) 2971–2981.

[22] P. Calvert, D. Duggal, P. Patra, A. Agrawal, A. Sawhney, Conducting polymer and conducting composite strain sensors on textiles, Mol. Cryst. Liq. Cryst. 484 (2008).

[23] DuPont, DuPont kapton HN polyimide film, Kapton HN datasheet (2011).

[24] Advanced Nano Products Silver Jet Ink, 2015. Available from: URL: http://anapro.com/eng/product/silver_inkjet_ink.html.

[25] Afga Specialities Products ORGACON™ Transparent Conductive Inkjet Ink: IJ-1005, 2013. Available from: URL: http://www.agfa.com/sp/global/en/binaries/IJ1005-2013v1.1_tcm611-86919.pdf.

[26] Y. Sun, S.P. Lacour, R.A. Brooks, N. Rushton, J. Fawcett, R.E. Cameron, Assessment of the biocompatibility of photosensitive polyimide for implantable medical device use, J. Biomed. Mater. Res. 90A (2009) 648–655.

[27] X. Crispin, F.L.E. Jakobsson, A. Crispin, P.C.M. Grim, P. Andersson, a Volodin, C. van Haesendonck, M. Van der Auweraer, W.R. Salaneck, M. Berggren, The origin of the high conductivity of poly(3, 4-ethylenedioxythiophene)-poly(styrenesulfonate) (PEDOT-PSS) plastic electrodes, Chem. Mater. 18 (2006) 4354–4360.

[28] Y. Liu, B. Weng, J.M. Razal, Q. Xu, C. Zhao, Y. Hou, S. Seyedin, R. Jalili, G.G. Wallace, J. Chen, High-performance flexible all-solid-state supercapacitor from large free-standing graphene–PEDOT/PSS films, Sci. Rep. 5 (2015) 17045.

[29] T. Öhlund, J. Örtegren, S. Forsberg, H.E. Nilsson, Paper surfaces for metal nanoparticle inkjet printing, Appl. Surf. Sci. 259 (2012) 731–739.

[30] F. Molina-Lopez, D. Briand, N.F. De Rooij, All additive inkjet printed humidity sensors on plastic substrate, Sens. Actuators B: Chem. 66–167 (2012) 212–222.

[31] M.L. Allen, M. Aronniemi, T. Mattila, A. Alastalo, K. Ojanperä, M. Suhonen, H. Seppä, Electrical sintering of nanoparticle structures, Nanotechnology 19 (2008) 175201.

[32] J.J.P. Valeton, K. Hermans, C.W.M. Bastiaansen, D.J. Broer, J. Perelaer, U.S. Schubert, G.P. Crawford, P.J. Smith, Room temperature preparation of conductive silver features using spincoating and inkjet printing, J. Mat. Chem 20 (2010) 543–546.
[33] R. Pallàs-Areny, J. Jordana, Ó. Casas, Optimal two-point static calibration of measurement systems with quadratic response, Rev. Sci. Instrum. 75 (2004) 5106–5111.

Biographies

Michela Borghetti received her Master's degree, *cum laude*, in Electronic Engineering from the University of Brescia in 2012. In 2015, she was visiting Ph.D. student at Universitat Politècnica de Catalunya. In 2016, She received the Ph.D. in Technology for Health from the University of Brescia. Now she is Postdoctoral Reasearcher with the Department of Information Engineering, University of Brescia. She is working on the design and fabrication of sensors for healthcare using low-cost technologies. Furthermore, she is developing electronic systems for measuring and monitoring limb movements.

Mauro Serpelloni is assistant professor of measurement at the Information Engineering Department. He received the Ph.D. in electronic instrumentation from the University of Brescia in 2006. From 2006–2010, he was Postdoctoral Researcher with the Department of Information Engineering, University of Brescia. Now he is Assistant Professor and Aggregate Professor with the Department of Information Engineering, University of Brescia. He has worked on several projects relating to the design, modelling, and fabrication of measurement systems for industrial applications. His research interests include electronic instrumentation, sensors, contactless transmissions between sensors and electronics and signal processing for microelectromechanical systems.

Emilio Sardini graduated in 1983 in Electronic Engineering from the Polytechnic of Milan. Since 1984 he conducts its research and teaching activities at the Department of Electronics for Automation, University of Brescia. Since 2006 he is full professor of Electrical and Electronic Measurement. He has done intensive research in the field of electronic instrumentation, sensors, and signal conditioning electronics. Recently, research has been addressed to the development of autonomous sensors for biomedical applications with some specific interest toward devices implantable inside the human body. He is author or coauthor of more than one hundred papers published on international journal.

Pandini, born in 1975 in Trento (Italy), studied Materials Engineering at the University of Trento, where he graduated. In his Ph.D. thesis he dealt with the time and temperature on the viscoelastic behavior of semicrystalline polymers at small and large deformations. Since 2005 is Assistant Professor in Materials Science and Technology at the University of Brescia. He has an expertise in the structural, mechanical and thermal characterization of polymeric and composite materials for engineering and biomedical applications. His fields of research mainly concerns the thermo-mechanical response of polymer-based functional materials (micro- and nano-structured polymer-based systems; nano-filled rubbers), and the shape memory behavior of tailored polymeric systems.